Calbindin D_{9k}: A Protein Optimized for Calcium Binding at Neutral pH†

Tõnu Kesvatera,[‡,§] Bo Jönsson,*[,||] Artur Telling,[§] Vello Tõugu,[§] Heiki Vija,[§] Eva Thulin,[‡] and Sara Linse[‡]

Departments of Biophysical Chemistry and Theoretical Chemistry, Lund University, P.O. Box 124, S-221 00 Lund, Sweden, and National Institute of Chemical Physics and Biophysics, Akadeemia tee 23, 12618 Tallinn, Estonia

Received July 6, 2001; Revised Manuscript Received October 12, 2001

ABSTRACT: The binding of calcium ions by EF-hand proteins depends strongly on the electrostatic interactions between Ca^{2+} ions and negatively charged residues of these proteins. We have investigated the pH dependence of the binding of Ca^{2+} ions by calbindin D_{9k}. This protein offers a unique possibility for interpretation of such data since the pK_a values of all ionizable groups are known. The binding is independent of pH between 7 and 9, where maximum calcium affinity is observed. An abrupt decrease in the binding affinity is observed at pH values below 7. This decrease is due to protonation of acidic groups, leading to modification of protein charges. The pH dependence of the product of the two macroscopic Ca^{2+}-binding constants can be formally described by the involvement of two acidic groups with pK_a = 6.6. Monte Carlo calculations show that the reduction of Ca^{2+} binding is strictly determined by variable electrostatic interactions due to pH-dependent changes not only in the binding sites, but also of the overall charge of the protein.

During the cell cycle in living organism, the hydrogen ion concentration (acidity), characterized by pH, varies and thereby regulates a variety of metabolic pathways. Allowances for pH changes, however, are rather limited—the intracellular pH is kept between 6.5 and 7.5, and crossing these limits is usually lethal.

The effects of hydrogen ions (H^+) and metal ions (M^{z+}) are often interrelated in biochemical processes and their physiological appearances. The uptake of protons and metal ions by chemical substances and biological macromolecules occurs via different mechanisms, and the relative contributions of interactions involved can be different. However, these processes have a common feature: they both result in change of the charge state of the compound to which they bind. Thus, when the electrostatic interactions dominate, proton and metal ion uptake may result in similar physiological effects.

Among a number of hydrogen and metal ion-dependent biochemical processes, regulatory functions of calmodulin, troponin C, and several other calcium-binding proteins depend on large conformational changes triggered by Ca^{2+} binding. The effects of Ca^{2+} and H^+ uptake by calmodulin (*1*) and calbindin D_{28k} (*2*) as well as Ca^{2+} and H^+ fluxes in a number of other cellular processes (*3*) are interrelated and may mimic each other. The interaction of calmodulin with calcineurin, both EF-hand proteins, can be initiated either by Ca^{2+} or by H^+, suggesting a combined effect between Ca^{2+} and H^+ (*1*). Also, the conformational changes of S100 proteins with increasing H^+ concentration are similar to those induced by Ca^{2+} binding (*4*). Calcium binding at pH 7.4 or a pH change from 7.4 to 5.6 were both found to decrease the Stokes radius of calmodulin (*5*).

Calmodulin-related proteins are adapted for high-affinity calcium binding, containing pairs of Ca^{2+} sites, so-called EF-hands (*6*). With few exceptions, the calcium-binding loop sequences are composed of 12 amino acids including up to 5 acidic residues. In most EF-hand sites, the bound Ca^{2+} ion is coordinated by six backbone and side chain oxygen atoms and by a water molecule (*7*). The binding of calcium ions to EF-hand sites is largely determined by electrostatic interactions. Neutralization of surface charges by mutations (*8*), as well as screening of electrostatic interactions by added inorganic salts or increasing the protein concentration, reduces the calcium affinity (*9*−*11*). If coordinating oxygen atoms are removed by point mutation, a drastic reduction in affinity is seen (*12*, *13*). However, the replacement of a negatively charged ligand by a neutral one (e.g., Asp→Asn) sometimes decreases and sometimes increases the Ca^{2+} affinity (*14*) because the reduced electrostatic attraction of the Ca^{2+} ion may be compensated by reduced repulsion among the coordinating groups. Thus, the calcium affinity of an EF-hand protein depends on the protonation state of acidic residues in a nontrivial way. For charged amino acid residues not participating in the binding of calcium ions, the behavior is as expected; i.e., neutralization of an acidic residue lowers the affinity.

The calcium affinity for calmodulin is fairly constant over a broad range around pH 7.5 (*15*). Calmodulin gradually loses bound calcium ions with decreasing pH at acidic values (on average 3 Ca^{2+} ions remain bound to calmodulin at pH 5, 2 Ca^{2+} bound at pH ∼4.3, 1 Ca^{2+} bound at pH ∼3.9), and the affinity for Ca^{2+} becomes negligible below pH 3.5,

† This work was supported by the Swedish Natural Science Research Council, The Royal Swedish Academy of Sciences, and the Estonian Science Foundation.

* Correspondence should be addressed to this author at the Department of Theoretical Chemistry, Lund University, P.O. Box 124, S-221 00 Lund, Sweden. E-mail: bo.jonsson@teokem.lu.se, fax: INT + 46 46 222 45 43, phone: INT + 46 46 222 82 39.

‡ Department of Biophysical Chemistry, Lund University.

§ National Institute of Chemical Physics and Biophysics.

|| Department of Theoretical Chemistry, Lund University.

10.1021/bi0114022 CCC: $20.00
Published on Web 11/20/2001

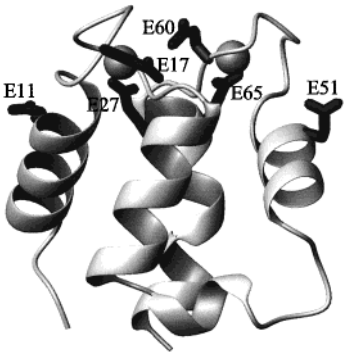

FIGURE 1: Outline of the three-dimensional structure of calbindin D_{9k}. Acidic side chains with pK_a values of 5.0 or higher are shown in black. Of the shown residues, E27 and E65 coordinate Ca^{2+} with their side chain carboxylates, and E11 and E60 with their backbone carbonyls. Figure prepared with the program MOLMOL (*20*).

as monitored by flow dialysis (*16*). Calcium-free calmodulin has been reported to bind protons with an estimated pK_a of 5.5 (*17*). Ca^{2+}-binding properties of the whiting albumin are independent of pH from 6 to 9 while the pH dependence of fluorometric characteristics of whiting parvalbumin shows pronounced changes to occur around pH 5.1 and 3.7. The first change probably results from the protonation of the carboxylate groups, which lowers their affinity for the calcium ions. The second transition is attributable to either acidic denaturation or dissociation of isoelectric aggregates (*18*).

It is usually assumed that all acidic residues in EF-hand proteins are negatively charged at neutral pH. Recent pK_a measurements confirm that aspartic and glutamic acid residues in apo-calbindin D_{9k} are predominantly unprotonated at this pH (*19*). However, several aspartic and glutamic acids in the calcium-binding area have unusually high pK_a values. Residues Glu17 and Glu27 at the N-terminal Ca^{2+} site manifest pK_a values of 6.5 and 6.4, and the side chain carboxyl group of Glu60, which is located between the two calcium sites (Figure 1), titrates with a pK_a of 6.2 (*19*). Changes in calcium affinity in the near-neutral pH range can bear regulatory implications.

In the present work, we have studied the effect of pH on the calcium affinity for calbindin D_{9k} (M_r 8500, 75 amino acids), a monomeric calcium-binding protein of the S100 family of the calmodulin-related proteins. It is present in the small intestine, placenta, and bone. It is assigned to the Ca^{2+} buffering and transport fraction of the superfamily of EF-hand proteins (*21*) and is involved in trans-cellular transport of Ca^{2+} ions (*22*, *23*). The protein contains two EF-hand calcium-binding sites: the C-terminal site is formed by a canonical 12-residue loop, and a variant 14-residue loop comprises the N-terminal site. Calbindin D_{9k} is outstandingly stable at various solvent conditions (*24*), and the three-dimensional structures have been determined for both the apo (*25*) and the holo (*26*, *27*) form. The pK_a values of all titratable groups in calbindin D_{9k} have been measured, offering a unique possibility for a detailed molecular interpretation of Ca^{2+} affinity variations in different pH intervals.

EXPERIMENTAL PROCEDURES

Materials. Wild-type calbindin D_{9k} was produced in *Escherichia coli* using a synthetic gene (*28*) and purified to homogeneity as previously described (*29*). Agarose gel electrophoresis, SDS−polyacrylamide gel electrophoresis, and ^{1}H NMR confirmed the purity of the protein preparation. Quin[1] 2 tetrapotassium salt was obtained from Fluka (Buchs, Switzerland), 5,5′-Br_2BAPTA tetrapotassium salt from Molecular Probes (Eugene, OR), and Chelex-100 from BioRad. Inorganic salts and buffers were of analytical grade.

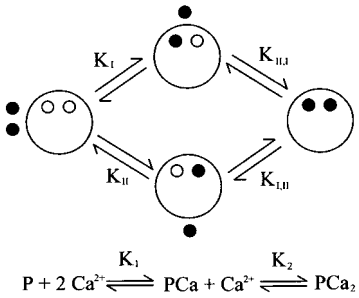

FIGURE 2: Definition of microscopic (top scheme) and macroscopic (bottom scheme) Ca^{2+}-binding constants.

Macroscopic Ca^{2+}-Binding Constants. Calcium binding to two individual sites (I and II) in a protein is characterized by four *microscopic* binding constants: K_I, K_{II}, $K_{I,II}$, and $K_{II,I}$. K_I and $K_{I,II}$ refer to Ca^{2+} binding to site I in the absence and presence, respectively, of Ca^{2+} in site II, while K_{II} and $K_{II,I}$ characterize site II at different calcium occupancy of site I. The *macroscopic* binding constants, K_1 and K_2, describe the binding of the first and second calcium ion, correspondingly, irrespective of which site is occupied (Figure 2).

$$K_1 = \frac{[PCa]}{[P][Ca^{2+}]} \text{ and } K_2 = \frac{[PCa_2]}{[PCa][Ca^{2+}]} \qquad (1)$$

[P] and [Ca^{2+}] are the concentrations of free protein and free calcium, and [PCa] and [PCa_2] are the concentrations of protein with one and two bound calcium ions, respectively. The macroscopic and microscopic binding constants are related as follows:

$$K_1 = K_I + K_{II} \qquad (2a)$$

$$K_2 = K_I K_{II,I}/(K_I + K_{II}) \qquad (2b)$$

$$K = K_1 K_2 = K_I K_{II,I} = K_{II} K_{I,II} \qquad (2c)$$

Experimentally, the total binding constant K can be determined at the higher confidence level than K_1 and K_2 since the binding of two Ca^{2+} ions to calbindin D_{9k} is characterized by strong positive cooperativity (*9*).

The two macroscopic binding constants were determined from titration of the protein with Ca^{2+} in the presence of a chromophoric chelator. The chelator was either Quin 2 or 5,5′-Br_2BAPTA, whose Ca^{2+}-binding constants were determined in separate experiments. The free calcium concentration in each buffer was kept below 1 μM by dialysis against Chelex-100. Protein and chelator concentrations were in the 12−25 μM range. The total volume in the cell was 2.5 mL, and 5 μL aliquots of $CaCl_2$ stock solution (3.0 or 10.0 mM) were added. The absorbance at 263 nm was recorded at each

[1] Abbreviations: 5,5′-Br_2BABTA, 5,5′-dibromo-1,2-bis(*o*-aminophenoxy)ethane-*N*,*N*,*N*′,*N*′-teraacetic acid; Quin, 2,2-[[bis[(carboxymethyl)-amino]-5-methylphenoxy]methyl]-6-methoxy-8-[bis(carboxymethyl)-amino]quinoline.

titration point. The dissociation constant of the chelator−Ca^{2+} complex, K_{DQ}, was calculated from the experimental data determined in the absence of protein by fitting the absorbance, A, at different total calcium concentrations (C_{Ca}) to the equation:

$$A = \{A_{max} + (A_{min} - A_{max})Y/(Y + K_{DQ})\}V/V_0 \quad (3)$$

where V and V_0 are the total volumes at the particular titration point and before adding the first $CaCl_2$ aliquot, respectively. A_{min} and A_{max} are the absorbances that the Ca^{2+}−chelator complex and free chelator, respectively, would have at no dilution. The free Ca^{2+} concentration, Y, was taken as the positive root of the equation:

$$C_{Ca} = Y + YC_Q/(Y + K_{DQ}) \quad (4)$$

where C_Q is the total chelator concentration.

The macroscopic binding constants, K_1 and K_2, of the protein were obtained by numerical fitting to the experimental points of titrations of protein−chelator mixtures as described earlier (*9*), using eq 3. In this case, the free Ca^{2+} concentration, Y, was solved using the Newton−Raphson method according to the equation:

$$Y = C_{Ca} - YC_Q/(Y + K_{DQ}) - \{C_P(K_1Y + 2K_1K_2Y^2)\}/(1 + K_1Y + K_1K_2Y^2) \quad (5)$$

where C_P is the total protein concentration.

The binding constants as a function of pH were fitted to the equation:

$$A_{lim}/A = 1 + (C_H/K_{a1})^n + K_{a2}/C_H \quad (6)$$

Equation 6 is commonly used to describe the activity of enzymes involved in acid−base equilibria, where the protonated or deprotonated forms are unable to bind substrate or perform catalysis. We are testing if the present data can be fitted using the same approach although we would expect involvement of all surface charges according to their proton uptake capacity. A stands for log (K_1K_2), log K_1, log K_2, or −log K_{DQ}, A^{lim} is the corresponding limiting (pH-independent) value, K_{a1} and K_{a2} are apparent ionization constants, C_H is the proton concentration, and n is the number of protons involved. The fitted quantities are in principle not interpretable in molecular terms, but can sometimes give a useful overall description of the binding process. The parameter n was taken equal to unity for fitting the pH dependence of K_{DQ}, since the fit was not improved when n was allowed to vary.

RESULTS AND DISCUSSION

The calcium-binding constants of calbindin D_{9k} were determined by monitoring the distribution of Ca^{2+} ions between the protein and a chromophoric chelator, as illustrated in Figure 3. The chelators Quin 2 and 5,5′-Br_2-BAPTA, suitably having calcium affinities similar to that of calbindin, both contain four carboxyl groups involved in calcium binding, and their affinities are pH-dependent as shown in Figure 4.

The measured macroscopic Ca^{2+}-binding constants, K_1 and K_1K_2 of calbindin D_{9k}, and the Ca^{2+} affinities for 5,5′-Br_2-BAPTA and Quin 2 are given in Table 1. The fitted parameters describing the observed pH dependencies according to eq 6 are summarized in Table 2. For the chelator, we find that the apparent proton dissociation constant pK_{a1} is equal to 6.05, which probably reflects the dissociation of the last carboxylic group in the chelator. The second constant, pK_{a2} = 10.7, could reflect the formation of calcium carbonate, since the sample was not protected against atmospheric carbon dioxide.

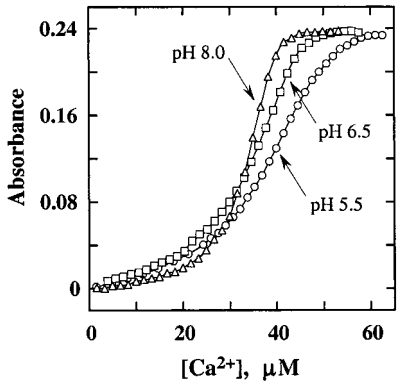

FIGURE 3: Normalized absorbances ($A_0 - A_{Ca}$) at 263 nm versus total Ca^{2+} concentration for titration of calbindin D_{9k} at 25 °C and variable pH in buffers containing 5 mM KCl and the chromophoric chelator 5,5′-Br_2BAPTA.

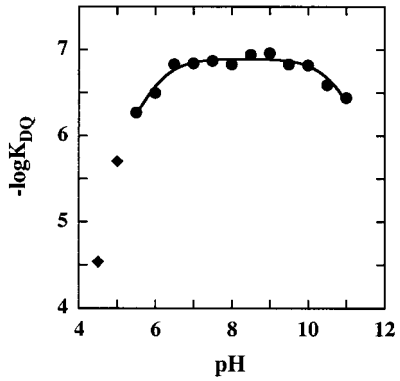

FIGURE 4: pH dependence of Ca^{2+} binding by the chelators 5,5′-Br_2BAPTA (●) and Quin 2 (◆) at 25 °C in buffers containing 5 mM KCl. The solid line for 5,5′-Br_2BAPTA corresponds to the fitted parameters in Table 2. The estimated upper limit of an error for K_{DQ}, K_1K_2, K_1, and K_2 is ±0.2 unit in the logarithmic scale.

Table 1: Calcium-Binding Constants for Calbindin D_{9k} and the Chromophoric Chelator 5,5′-Br_2BAPTA or Quin 2* at 25 °C[a]

pH	buffer	K_1K_2 ($\times 10^{-12}$ M^2)	K_1 ($\times 10^{-6}$ M)	K_{DQ} ($\times 10^6$ M^{-1})
4.5	MES	0.41	−	29*
5.0	MES	9.67	6.20	1.98*
5.5	MES	198.7	17.25	0.535
6.0	MES	334	27.5	0.318
6.5	MES	4596	84.8	0.147
7.0	MOPS	8180	103	0.146
7.5	MOPS	16100	135	0.137
7.5	Tris	18300	158	0.132
8.0	Tris	17200	147	0.123
8.0	taurine	6542	101	0.168
8.5	taurine	12600	101	0.114
9.0	taurine	14200	169	0.110
9.5	taurine	6300	94.0	0.148
10.0	Lys	11900	122	0.150
10.5	Lys	3060	40.6	0.225
11.0	Lys	3930	104	0.361

[a] The KCl concentration is 5 mM.

Table 2: Fitted Parameters According to Eq 6

A	A^{lim}	pK_{a1}	n	pK_{a2}	r
log (K_1K_2)	16.07 ± 0.10	6.59 ± 0.15	2.02 ± 0.18	10.48 ± 0.31	0.988
log K_1	8.07 ± 0.07	6.36 ± 0.29	0.94 ± 0.23	11.20 ± 0.47	0.939
log K_2	8.01 ± 0.06	6.52 ± 0.18	1.14 ± 0.16	10.80 ± 0.23	0.977
−log K_{DQ}	6.90 ± 0.02	6.05 ± 0.07	1	10.67 ± 0.09	0.970

Electrostatic interactions between Ca^{2+} ions and negatively charged side chains of acidic residues provide substantial contributions to the free energy of calcium binding to calbindin (*9*) and calmodulin (*30*) as well as other related proteins. Studies using charge-deletion mutations have demonstrated that the electrostatic contribution depends strictly on the distance of an ionic site of a protein from the bound Ca^{2+} ions and on the concentration of a screening factor such as inorganic salt (*10*) or protein (*11*). In addition to purely electrostatic factors, the dramatic loss of Ca^{2+}-binding capacity of EF-hand proteins upon the substitutions at key chelating positions, however, results from disturbances of the metal coordination sphere. This disturbance of the coordination sphere is difficult to model using dielectric continuum approaches. The long-range electrostatic interactions, on the other hand, are almost quantitatively described by continuum electrostatics, provided a high dielectric permittivity is assumed for the protein interior (*10*). One should note that there is a significant difference between the calculation of binding constant shifts, e.g., for binding of calcium ions to proteins, and the calculation of pK_a shifts of titrating amino acid residues. In the latter case, one is comparing the behavior of a free amino acid with the same residue in a protein. Thus, the change in the environment is quite large. In the case of calcium binding, one compares the different binding affinities of the same protein under different external conditions (salt, pH, etc.) or arising as a consequence of mutations of selected amino acid residues.

The pH-dependent calcium-binding measurements in the present study were performed at low enough ionic strength in order to minimize screening effects and maintain maximum possible electrostatic interactions. Due to the high negative net charge of calbindin in the neutral pH range, however, the chemical potential of free calcium ions is very sensitive to both salt and protein concentration at low salt content (*15*). Therefore, in the absence of added salt, small ionic strength variations upon mixing the Ca^{2+} titration medium in different buffer systems as well as changes in ionic strength due to added Ca^{2+} ions lead to numerical difficulties in the interpretation of experimental data. We have found that 5 mM KCl is sufficient to minimize these effects and to provide acceptable reproducibility of the measured binding parameters over the studied pH range from 4.5 to 11. Parallel measurements in different buffers were made in order to even out the observed minor buffer-specific effects so as not to impair the conclusions.

The pH dependence of log (K_1K_2) in a buffer containing 5 mM KCl has a wide optimum, ranging from pH 7 to 9 (Figure 5). Curve-fitting according to eq 6 yields two apparent pK_a values, 6.6 and 10.5, for the data in Figure 5. The former protonization, which according to the fit involves two protons, probably reflects the dissociation of acidic groups in the calcium-binding sites. Strongly upshifted pK_a's of Glu 17, Glu 27, and Glu 60, which have recently been determined from NMR experiments to be 6.4, 6.5, and 6.2, respectively (*19*), are possible candidates (Table 2).

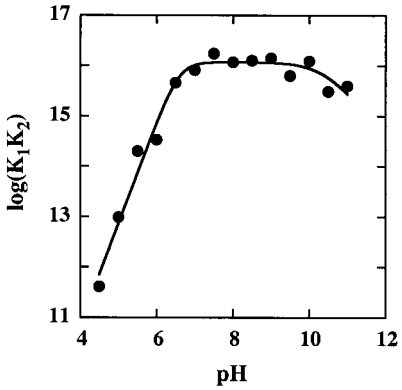

FIGURE 5: pH dependence of log (K_1K_2) for Ca^{2+} binding by calbindin D_{9k} at 25 °C in buffers containing 5 mM KCl. The solid line corresponds to the fitted parameters in Table 2.

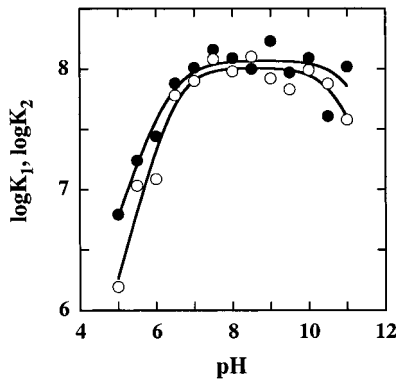

FIGURE 6: pH dependence of log K_1 (●) and log K_2 (○) for Ca^{2+} binding by calbindin D_{9k} at 25 °C. Solid lines correspond to the fitted parameters in Table 2.

Macroscopic equilibrium constants for the binding of the first (K_1) and the second (K_2) calcium ions in Figure 6 show similar pH dependencies. The fitted pK_a values for both K_1 and K_2 (Table 2) are similar to those observed for the total binding constant for two Ca^{2+} ions, except that one proton is apparently involved in each protonation. Manifestation of similar pK_a's in the macroscopic Ca^{2+}-binding constants is an expected result because according to eq 2 they all depend on the microscopic binding constants for both sites. That is, if each of the binding sites is affected by one titratable group, one should expect the results shown in Table 2. Note, however, that the experimental data for the individual binding constants K_1 and K_2 are numerically less reliable than their product.

The upper apparent pK_a of 10.5 is similar to that found for the chelator, which supports our conclusion that it is an artifact coming from dissolved CO_2. Another possible explanation for the observed decay in binding constants above pH 10 is caused by the titration of lysine residues. Several lysines, Lys1, -16, -25, and -71, are known to titrate in this regime both in the apo form and in calcium-loaded calbindin (*31*). Thus, the decrease in calcium affinity at high pH may result from structural disturbances in the calcium coordination spheres caused by deprotonation of lysine residues. We believe, however, that the formation of calcium carbonate is a more likely explanation, as it also explains the pH dependence for the chelator.

To gain further insight into the calcium-binding process, we performed theoretical modeling of the binding of two Ca^{2+} ions ($K = K_1K_2$) to calbindin at variable pH. The free energy change associated with the transfer of two Ca^{2+} ions from the solution to the binding sites of calbindin includes several components: direct interaction with calcium-coordinating oxygen atoms, contributions due to hydration, long-range electrostatic interactions with protein charges, etc. Since variation of pH alters the net charge of a protein, its major effect concerns both the short- and the long-range electrostatic contributions to the free energy change associated with Ca^{2+} binding, ΔG_{el}. With short-range effects, we mean the titration of charged ligands in the binding sites, and long-range electrostatic effects come from nonligands.

The difference in the electrostatic free energy of the bound and free calcium states, ΔG_{el}, can be described in terms of relative changes in the macroscopic binding constants with respect to the pH chosen as a reference state:

$$K/K^{ref} = \exp[-(\Delta G_{el} - \Delta G_{el}{}^{ref})/k_BT] \qquad (7)$$

where k_B is the Boltzmann constant and T is the absolute temperature. In other words, we are measuring the change in activity coefficients between two states. The electrostatic contribution, ΔG_{el}, can also be expressed as

$$\Delta G_{el} = \mu^{ex}(2Ca^{2+},B) - 2\mu^{ex}(Ca^{2+},F) \qquad (8)$$

where $\mu^{ex}(2Ca^{2+},B)$ and $\mu^{ex}(Ca^{2+},F)$ are the excess chemical potential for two bound and free calcium ions, respectively. The excess free energy of any species can be obtained through a perturbation procedure, usually referred to as Widom's test particle's technique (*33*). To calculate μ^{ex}-(Ca^{2+},F), an appropriate test particle is inserted randomly over the simulation cell. The excess chemical potential is then calculated as

$$\beta\mu^{ex} = -\ln \langle \exp(-\beta\Delta U(\mathbf{r}^N,\mathbf{r}_T)\rangle_0$$

where $\Delta U(\mathbf{r}^N,\mathbf{r}_T)$ is the interaction energy between the test particle at position $\mathbf{r}_T$ and all other particles in the system. The subscript $\langle ... \rangle_0$ indicates that the ensemble average is calculated over the unperturbed system, which has also been corrected for the finite system size (*34*). That is, all types of insertions can be made in a single simulation. The chemical potential of a bound calcium ion is calculated simply by inserting a test particle into a binding site. We calculated the values of $\mu^{ex}(2Ca^{2+},B)$ and $\mu^{ex}(Ca^{2+},F)$ over the pH range using Monte Carlo simulations in a semigrand canonical ensemble assuming a fixed protein structure determined for the crystalline state (*26*). In principle, it would be more correct to use a solution structure from NMR studies. In practice, however, this is nontrivial since the NMR structure is not one single well-defined protein conformation, but a collection of configurations, whose statistical weights are unknown (*27*). Comparing the NMR structures to the structure obtained from X-rays shows only minor differences (*27*), and the same is true for the apo and calcium-loaded forms according to NMR studies (*25*).

It is important to note that the theoretical procedure for calculating binding constant shifts is relatively insensitive to structural changes. This is true as long as the structural changes are approximately the same in the two states that are compared; i.e., the structural response to Ca^{2+} binding is the same at two different pH values. ΔG_{el} and $\Delta G_{el}{}^{ref}$ can both contain significant contributions from structural changes, which fortunately cancel when calculating the difference in eq 7. Traditionally, the approach to electrostatic interactions in proteins has been via the Debye−Hückel theory or in a few cases the nonlinear Poisson−Boltzmann equation. Monte Carlo simulations offer an efficient alternative that avoids the approximations inherent in these other methods. That is, both nonlinear effects and ion−ion correlations are properly accounted for in the simulations.

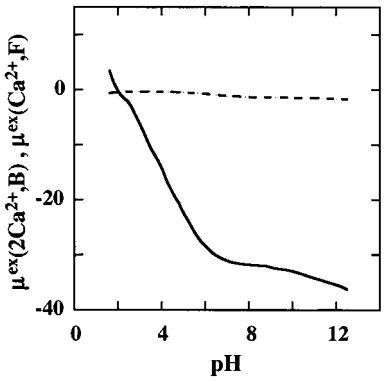

FIGURE 7: Excess chemical potentials for two calcium ions (units of kT) as a function of pH. Solid line, bound; dashed line, free. Calculations are based on the crystallographic structure of $(Ca^{2+})_2$-calbindin D_{9k} (*26*).

Variations in the protein net charge with changing pH were calculated according to the procedures previously used in modeling the pK_a values of ionizable groups in calbindin (*19*, *32*). Altogether 31 simulations at different pHs were performed. At each pH, the average fractional occupancies of all titrating groups were calculated. The excess chemical potentials of bound and free calcium ions were obtained from a modified Widom perturbation technique (*33*, *34*). The pH dependencies of calculated excess chemical potentials are illustrated in Figure 7.

The excess chemical potential of the two bound Ca^{2+} ions, $\mu^{ex}(2Ca^{2+},B)$, changes dramatically at acidic pH, where the glutamates and aspartates successively ionize with increasing pH. $\mu^{ex}(2Ca^{2+},B)$ passes a plateau around neutral pH, whereupon it starts to decrease again due to titrating lysine residues. The decrease is not as rapid as on the acidic side, mainly because the lysines are on average further away from the binding sites than the acidic residues. There is also a stronger electrostatic screening from the counterions at high pH due to nonlinear effects and also ion−ion correlations.

As compared to the bound state, the change in excess chemical potential of free Ca^{2+} ions, $\mu^{ex}(Ca^{2+},F)$, is small but characteristically dependent on the net charge of the protein, as illustrated in Figure 8. In particular, one can note the decay in $\mu^{ex}(Ca^{2+},F)$ at high pH. When the net charge on calbindin becomes strongly negative, then the chemical potential of free calcium ions decreases significantly. This is in contrast to the acidic side between pH 2 and 5, where $\mu^{ex}(Ca^{2+},F)$ is approximately independent of the protein charge. This is a general phenomenon, which for sufficiently highly charged macromolecules can lead to counterintuitive results; the negatively charged protein becomes a less efficient complexing agent for cations at high pH despite

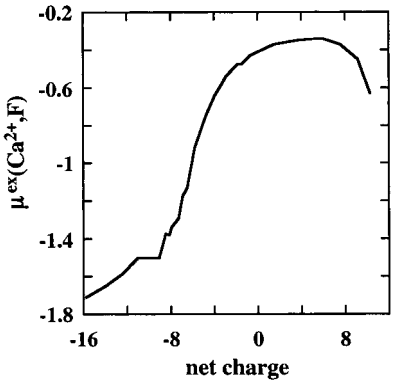

FIGURE 8: Dependence of the excess chemical potential for a free calcium ion (units of kT) on the net charge of calbindin D_{9k}.

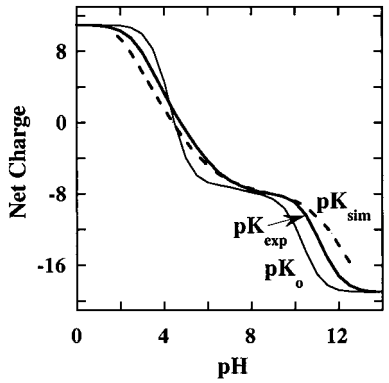

FIGURE 9: Full titration curves for apo-calbindin D_{9k} as calculated using experimental (thick), theoretical (dashed), and model compound (thin) pK_a values for ionizable groups. A distinct plateau is seen around physiological pH.

the increasing negative charge. Unfortunately, this feature is not captured in the present experiment, where the binding constant is, due to its strength, only determined indirectly via a competition procedure with the chelator (*35*). This also prevents a direct comparison between experiment and simulations for the high-pH range, notably above 10.

The experimental net charge is calculated using data for the titration behavior of all ionizable groups, including Tyr13 and N-terminal NH_2 (unpublished data), obtained by NMR measurements (*19*, *31*, *32*). The theoretical net charge is calculated directly in the simulations as the sum of average fractional charges on titrating sites. The comparison in Figure 9 shows good agreement over the pH range, where the protein net charge varies from +9 to −16. The assumption of ideal behavior, i.e., assuming unperturbed pK's for all titrating groups, gives a significantly different net charge behavior.

Shifts in log (K_1K_2) due to changing pH (protein net charge) were calculated as $\Delta \log (K_1K_2) = [\mu^{ex}(2Ca^{2+},B) - 2\mu^{ex}(Ca^{2+},F)]/\ln (10)$. To compare the measured and calculated log (K_1K_2) values, they were normalized relative to pH 8, the experimental optimum for calcium affinity. The agreement between theory and experiment is excellent, as illustrated in Figure 10. The calculations assume that shifts in calcium-binding constants are due to pH-dependent variation of the degree of overall proton uptake by ionization sites in calbindin D_{9k}. It has to be concluded that pH-dependent variation in the overall calcium affinity is not caused by proton uptake by a few specific acidic residues at the binding sites. The electrostatic contribution to the free

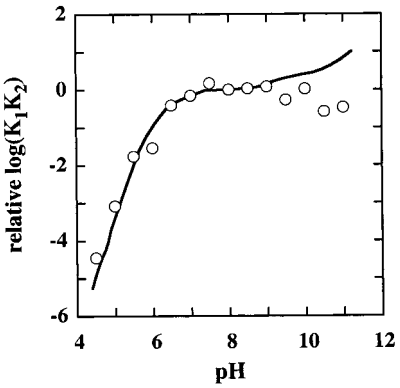

FIGURE 10: Experimental and simulated log (K_1K_2) shifts relative to pH 8.

energy of calcium binding decreases due to reduction of the net negative charge at acidic pH. According to the Coulomb's law, ionic charges at the binding sites are the largest contributors as they are generally located at the shortest distances from the bound calcium ions. In agreement with this, the proton uptake by residues Glu17 and Glu27 marks the onset of the reduction in calcium affinity. However, the further decrease of calcium-binding constants with increasing H^+ concentration depends on the reduction of the overall negative charge of the protein due to protonation of other acidic residues as well.

The reduced Ca^{2+} affinity due to protonation of acidic side chains correlates well with mutational studies in which acidic residues were replaced by neutral ones, leading to reduced Ca^{2+} affinity and reduced Ca^{2+} association rate (*8*, *9*, *36*). In the calmodulin-like proteins, the accumulation of negative charges in the binding area accelerates the association rate for Ca^{2+} to the diffusion-controlled regime to enable a rapid response during Ca^{2+} signaling events. However, accumulation of many negatively charged groups leads to structural destabilization (*37*). Our data show that addition of a single proton is enough to reduce the affinity; hence, the proteins seem to have accumulated just enough charge to reach the diffusion-controlled limit. Conditions of cellular Ca^{2+} overload are often accompanied by acidosis, and pH drops below 7. Due to the elevated pK_a values, this drop in pH leads to protonation, and the signaling proteins may lose there ability to respond appropriately to Ca^{2+} signals. One may speculate that this imbalance accelerates the processes leading to programmed cell death during conditions of Ca^{2+} overload and acidosis.

It is seen in Figure 10 that the simulated calcium-binding constant is close to its optimum at around pH 8. A further increase of the protein charge only leads to a marginal increase in the binding constant. Several factors contribute to this behavior: (i) additional negative charges (or, more correctly, removal of positive ones) are placed far away from the binding sites; (ii) the chemical potential of free calcium ions decreases; and (iii) nonlinear electrostatic effects as well as ion−ion correlations cause additional screening, which eventually will make addition of further negative charges counterproductive.

Unfortunately, at alkaline pH above 10, the results of our measurements may suffer from the presence of CO_2. Even if this practical complication can be removed, the comparison with theoretical calculations at high pH is still hampered by

the fact that the experimental K_1K_2 is only determined indirectly via the chelator. The comparison could of course be carried out, provided the simulations actually mimicked the experimental situation more faithfully. This amounts to replacing, in eq 8, the excess chemical potential for free calcium ions measured in the protein solution by the corresponding quantity measured in the appropriate chelator solution.

Perspectives of pK_a Measurements for the Ca^{2+}-Loaded Calbindin. The present study shows an abrupt decrease in the calcium affinity for calbindin at pH below 7. At pH 4.5, this results in a decrease of more than 4 orders of magnitude in the product of binding constants for two calcium ions. To measure the pK_a's of all acidic residues in the calcium-loaded form of calbindin, a significant amount of Ca^{2+} has to be added to ensure an excess of Ca^{2+} over the full titration range down to at least pH 2. It is still questionable that Ca^{2+} would remain bound when the chelating side chains are protonated. The added Ca^{2+} will, however, increase the ionic strength and result in significant screening of electrostatic interactions which are the major determinant of pK_a shifts from their standard values. Consequently, the measurable pK_a shifts for the calcium-loaded calbindin will be much smaller than those obtained for the apo form at low ionic strength. Also, because of the different ionic strength conditions, the pK_a values for the apo and holo forms would be difficult to compare.

CONCLUSION

Calbindin D_{9k} is optimized for high-affinity calcium binding at neutral pH. The calcium affinity, however, is very sensitive to pH changes in the allowed intracellular range below pH 7 due to acidic groups with highly elevated pK_a's on the protein surface. Thus, the interrelated uptake of Ca^{2+} and H^+ ions can be a significant regulatory factor for intracellular calcium buffering and transport functions of calbindin. The pH variation of calcium binding can be almost quantitatively described using a dielectric continuum model for electrostatic interactions.

REFERENCES

1. Huang, S., Carlson, G. M., and Cheung, W. Y. (1994) *J. Biol. Chem. 269*, 7631−7638.
2. Berggård, T., Silow, M., Thulin, E., and Linse, S. (2000) *Biochemistry 39*, 6864−6873.
3. Busa, W. B., and Nuccitelli, R. (1984) *Am. J. Physiol. 246*, 409−438.
4. Baudier, J., and Gerard, D. (1986) *J. Biol. Chem. 261*, 8204−8212.
5. Sorensen, B. R., and Shea, M. A. (1998) *Biochemistry 37*, 4244−4253.
6. Kretsinger, R. H., and Nockolds, C. E. J. (1973) *J. Biol. Chem. 248*, 3313−3326.
7. Strynadka, N. C. J., and James, M. N. G. (1989) *Annu. Rev. Biochem. 58*, 951−988.
8. Linse, S., Brodin, P., Johansson, C., Thulin, E., Grundström, T., and Forsén, S. (1988) *Nature 335*, 651−652.
9. Linse, S., Johansson, C., Brodin, P., Grundström, T., Drakenberg, T., and Forsén, S. (1991) *Biochemistry 30*, 154−162.
10. Kesvatera, T., Jönson, B., Thulin, E., and Linse, S. (1994) *Biochemistry 33*, 14170−14176.
11. Linse, S., Jönsson, B., and Chazin, W. J. (1995) *Proc. Natl. Acad. Sci. U.S.A. 92*, 4748−4752.
12. Maune, J. F., Klee, C. B., and Beckingham, K. (1992) *J. Biol. Chem. 267*, 5286−5295.
13. Carlström, G., and Chazin, W. J. (1993) *J. Mol. Biol. 231*, 415−430.
14. Waltersson, Y., Linse, S., Brodin, P., and Grundström, T. (1993) *Biochemistry 32*, 7866−7871.
15. Svensson, B., Jönsson, B., Thulin, E., and Woodward, C. E. (1993) *Biochemistry 32*, 2828−2834.
16. Haiech, J., Klee, C. B., and Demaille, J. G. (1981) *Biochemistry 20*, 3890−3897.
17. Williams, R. J. P. (1992) *Cell Calcium 13*, 355−362.
18. Permyakov, E. A., Yarmolenko, V. V., Emelyanov, V. I., Burstein, E. A., Closset, J., and Gerday, C. (1980) *Eur. J. Biochem. 109*, 307−315.
19. Kesvatera, T., Jönsson, B., Thulin, E., and Linse, S. (2001) *Proteins: Struct., Funct., Genet. 45*, 129−135.
20. Koradi, R., Billeter, M., and Wütrich, K. (1996) *J. Mol. Graphics 14*, 51−55.
21. Ikura, M. (1996) *Trends Biochem. Sci. (Pers. Ed.) 21*, 14−17.
22. Chistiakos, S., Gabrielides, C., and Rhoten, W. B. (1989) *Endocr. Rev. 10*, 3−26.
23. Walters, J. R., Howard, A., Charpin, M. V., Gniecko, K. C., Brodin, P., Thulin, E., and Forsén, S. (1990) *Biochem. Biophys. Res. Commun. 170*, 603−608.
24. Wendt, B., Hofmann, T., Martin, S. R., Bayley, P., Brodin, P., Grundström, T., Thulin, E., Linse, S., and Forsén, S. (1988) *Eur. J. Biochem. 175*, 439−445.
25. Skelton, N. J., Kördel, J., and Chazin, W. J. (1995) *J. Mol. Biol. 249*, 441−462.
26. Szebenyi, D. M. E., and Moffat, K. (1986) *J. Biol. Chem. 261*, 8671−8777.
27. Kördel, J., Skelton, N. J., Akke, M., and Chazin, W. J. (1993) *J. Mol. Biol. 231*, 711−734.
28. Brodin, P., Drakenberg, T., Thulin, E., Forsén, S., and Grundström, T. (1989) *Protein Eng. 2*, 353−358.
29. Johansson, C., Brodin, P., Grundström, T., Thulin, E., Forsén, S., and Drakenberg, T. (1990) *Eur. J. Biochem. 187*, 455−460.
30. Linse, S., Helmersson, A., and Forsén, S. (1991) *J. Biol. Chem. 266*, 8050−8054.
31. Kesvatera, T., Jönsson, B., Thulin, E., and Linse, S. (1996) *J. Mol. Biol. 259*, 828−839.
32. Kesvatera, T., Jönsson, B., Thulin, E., and Linse, S. (1999) *Proteins: Struct., Funct., Genet. 37*, 106−115.
33. Widom, B. (1963) *J. Chem. Phys. 39*, 2808−2812.
34. Svensson, B., Jönsson, B., and Woodward, C. E. (1988) *Mol. Phys. 64*, 247−259.
35. Da Silva, F. L. B., Jönsson, B., and Penfold, R. (2001) *Protein Sci. 10*, 1415−1425.
36. Martin, S. R., Linse, S., Johansson, C., Bayley, P. M., and Forsén, S. (1990) *Biochemistry 29*, 4188−4193.
37. Akke, M., and Forsén, S. (1990) *Proteins: Struct., Funct., Genet. 8*, 23−29.

BI0114022